Naval Research Laboratory

Washington, DC 20375-5000

AD-A276 509

NRL Memorandum Report 6777

Multimode Analysis of Bragg Reflectors for Cyclotron Maser Applications

ROBERT B. MCCOWAN,* ARNE W. FLIFLET AND
STEVEN H. GOLD

Beam Physics Branch
Plasma Physics Division

**Present Address: Advanced Technology Group, Varian Assoc, Inc., Beverly, MA*

February 16, 1991

94-06207

Approved for public release; distribution unlimited.

2 24 170

REPORT DOCUMENTATION PAGE

Form Approved OMB No. 0704-0188

1. AGENCY USE ONLY *(Leave blank)*

2. REPORT DATE
1991 February 16

3. REPORT TYPE AND DATES COVERED
Interim

4. TITLE AND SUBTITLE
Multimode Analysis of Bragg Reflectors for Cyclotron Maser Applications

5. FUNDING NUMBERS
ONR
47-3046-0-1

6. AUTHOR(S)
Robert B. McCowan,* Arne W. Fliflet and Steven H. Gold

7. PERFORMING ORGANIZATION NAME(S) AND ADDRESS(ES)
NRL
Washington, DC 20375-5000

8. PERFORMING ORGANIZATION REPORT NUMBER
NRL Memorandum Report 6777

9. SPONSORING/MONITORING AGENCY NAME(S) AND ADDRESS(ES)
ONR
Arlington, VA 22217

10. SPONSORING/MONITORING AGENCY REPORT NUMBER

11. SUPPLEMENTARY NOTES
*Present Address: Advanced Technology Group, Varian Assoc., Inc., Beverly, MA

12a. DISTRIBUTION/AVAILABILITY STATEMENT
Approved for public release; distribution unlimited.

12b. DISTRIBUTION CODE

13. ABSTRACT *(Maximum 200 words)*
Bragg reflectors are studied for application to mm-wave CARM oscillator resonators. The effects of mode coupling into undesired "stray" modes on reflectivity is investigated. A set of general equations for the coupled modes of rippled-wall resonators is derived. These equations can be solved using matrix-algebra techniques. The method of this paper is then applied to two cases, a TE_{11}, 85 GHz Bragg resonator, and a TE_{61}, 100 GHz Bragg resonator.

14. SUBJECT TERMS
Cyclotron maser
CARM
Bragg

15. NUMBER OF PAGES
19

16. PRICE CODE

17. SECURITY CLASSIFICATION OF REPORT	18. SECURITY CLASSIFICATION OF THIS PAGE	19. SECURITY CLASSIFICATION OF ABSTRACT	20. LIMITATION OF ABSTRACT
UNCLASSIFIED	UNCLASSIFIED	UNCLASSIFIED	SAR

NSN 7540-01-280-5500

Standard Form 298 (Rev 2-89)
Prescribed by ANSI Std Z39-18
298-102

CONTENTS

MULTIMODE ANALYSIS OF BRAGG REFLECTORS FOR CYCLOTRON MASER APPLICATIONS

I. INTRODUCTION

The cyclotron auto-resonance maser (CARM) is a promising source of high power radiation in the 100 GHz to 500 GHz frequency range that may impact the requirements of advanced systems for applications such as radar systems, communications systems and plasma heating. The requirements for guide magnetic field strength and electron energy in a CARM are advantageous when compared with competing devices. Compared with a gyrotron, the required magnetic field strength requirement is reduced because of the Doppler shift of the radiation.

Because the CARM depends on a convective instability, CARM oscillator operation must take place in a cavity that provides feedback of the radiation onto the electron beam. For typical CARM operation, the resonator reflectors must provide high reflectivity for modes that are far from cutoff. Mode selectivity is desirable, preferably with discrimination between modes differing in either transverse or axial structure. Modes that are near cutoff must be suppressed in order to minimize competition from the gyrotron interaction. Finally, the CARM cavity must allow unrestricted passage of an electron beam parallel to the axis.

CARM resonator reflectors may be achieved by using a small periodic corrugation of the waveguide surface. Each ripple provides a small reflection of wave amplitude. If the corrugation period is such that the radiation reflected from each of the corrugations adds in phase, the corrugated section can be highly reflective, and is known as a Bragg reflector[1]. This paper treats the reflection due to rippled wall sections as a mode conversion from a forward wave to a backward wave, with an approach to the analysis that is similar to the analyses of other mode converters[2]. Mode conversion from the desired mode to parasitic modes in the corrugated section is included in the analysis. A CARM oscillator with a Bragg resonator is illustrated in figure 1.

Manuscript approved November 28, 1990.

Previous work on Bragg reflectors has focused on a single mode approach to the reflection calculations[1, 3]. Palmer[4] examines the effects of multiple modes; however, his derivation requires that the coupled differential equations for the mode amplitudes be solved numerically. This paper presents a method of solving the coupled mode equations that only requires inversion of a single 4 by 4 complex matrix.

II. DERIVATION OF THE COUPLED-MODE EQUATIONS

The general case of waveguides with cross sections that change along the axis has been treated by Solymar[2], who formulated the equations governing the waveguide modes as a set of coupled differential equations for the wave amplitude, the "generalized telegraphist's" equations. The set of equations consists of two equations for each waveguide mode: each equation describes the amplitude of either the forward or the backward component of one waveguide mode.

$$\frac{\partial A_i^+}{\partial z} = -ik_i A_i^+ - \frac{1}{2}\frac{\partial(\ln K_i)}{\partial z} + \sum_p \left(S_{ip}^+ A_p^+ + S_{ip}^- A_p^-\right) \qquad \text{1a}$$

$$\frac{\partial A_i^-}{\partial z} = ik_i A_i^- + \frac{1}{2}\frac{\partial(\ln K_i)}{\partial z} + \sum_p \left(S_{ip}^+ A_p^- + S_{ip}^- A_p^+\right) \qquad \text{1b}$$

where A_i is the amplitude of the ith waveguide mode, k is the wave number of the mode, K is the wave impedance of the mode, and S is a wave-wave coupling coefficient. The designations $^+$ and $^-$ signify forward and backward going components, while the sum p is over all waveguide modes.

Equations 1a and b can be written in a slowly-varying-amplitude form by writing $A_i^{\pm}(z) = b_i^{\pm}(z)e^{\mp ik_i z}$.

$$\frac{\partial b_i^+}{\partial z} = -\tfrac{1}{2}\frac{\partial(\ln K_i)}{\partial z} + \sum_p \left\{ S_{ip}^+ b_p^+ e^{i(-k_p+k_i)z} + S_{ip}^- b_p^- e^{i(k_p+k_i)z} \right\} \qquad 2a$$

$$\frac{\partial b_i^-}{\partial z} = +\tfrac{1}{2}\frac{\partial(\ln K_i)}{\partial z} + \sum_p \left\{ S_{ip}^+ b_p^- e^{-i(-k_p+k_i)z} + S_{ip}^- b_p^- e^{-i(k_p+k_i)z} \right\} \qquad 2b$$

The coefficient of the term due to the impedance variation is the z derivative of the logarithm of the wave impedance.

$$\frac{\partial}{\partial z}\ln K = \frac{\partial}{\partial z}\ln(\omega/k) = -\frac{1}{k}\frac{\partial k}{\partial z} \qquad 3$$

where ω is the angular frequency of the radiation.

If a sinusoidal-profile rippled wall reflector is chosen,

$$\frac{\partial}{\partial z}a(z) = -\ell_0 k_B \sin(k_B z - \phi) \qquad 4$$

the wave impedance term K becomes

$$\frac{\partial}{\partial z}\ln K = \frac{\ell_0 k_B x_{mn}'^2}{k^2 a^3}\sin(k_B z - \phi) \qquad 5$$

$$S_{ip}^{-} = \frac{-k_B \ell_0 \sin(k_B z)\left[\frac{\sqrt{k_i}}{\sqrt{k_p}} x_p'^2\left(x_i'^2 - m^2\right) - \frac{\sqrt{k_p}}{\sqrt{k_i}} x_i'^2\left(x_p'^2 - m^2\right)\right]}{a\sqrt{x_i'^2 - m^2}\sqrt{x_p'^2 - m^2}\left(x_i'^2 - x_p'^2\right)} \tag{6}$$

for TE-TE coupling,

$$S_{ip}^{-} = \frac{-m\omega k_B \ell_0 \sin(k_B z)}{ac\sqrt{k_i k_p}\left(x_i'^2 - m^2\right)} \tag{7}$$

for TE-TM coupling, and

$$S_{ip}^{-} = \frac{-k_B \ell_o \left(k_i x_p^{\,2} - k_p x_i^{\,2}\right)\sin k_B z}{a\sqrt{k_i k_p}\left(x_p^{\,2} - x_i^{\,2}\right)} \tag{8}$$

for TM-TM coupling.

Equations 2 can be simplified with the transformation

$$b_i^{\pm} = f_i e^{\pm i\frac{\Delta}{2}z} \tag{9}$$

to arrive at the following expression for the mode amplitudes.

$$\frac{\partial f_i^{+}}{\partial z} = i\frac{\Delta_{ii}}{2} f_i^{+} - G_{ii}^{-} f_i^{-} + \sum_{p \neq i} H_{ip}^{-} f_p^{-} \tag{10a}$$

$$\frac{\partial f_i^{-}}{\partial z} = -i\frac{\Delta_{ii}}{2} f_i^{-} + G_{ii}^{-} f_i^{+} - \sum_{p \neq i} H_{ip}^{-} f_p^{+}, \tag{10b}$$

Where G is the combination of the impedance term and the wall current term, and

$$\begin{aligned} \Delta_{ii} &= 2k_i - k_B \\ \Delta_{ip} &= k_i + k_p - k_B \\ \Delta_{pp} &= 2k_p - k_B \end{aligned} \quad . \tag{11}$$

For TE modes,

$$G = \frac{l_0}{2}\left\{\frac{x'^4_{mn} - m^2 a^2\left(\omega^2 / c^2 + k^2\right)}{k a^3\left(x'^2_{mn} - m^2\right)}\right\}, \tag{12}$$

and

$$G = \frac{l_0}{2a}\frac{\omega^2/c^2 + k^2}{k} \tag{13}$$

for the TM modes[1]. H_{ip} is the cross mode coupling term, and is

$$H_{ip} = \frac{\ell_o k_B\left(x'^2_p\left(x'^2_i - m^2\right)\frac{\sqrt{k_i}}{\sqrt{k_p}} - x'^2_i\left(x'^2_p - m^2\right)\frac{\sqrt{k_p}}{\sqrt{k_i}}\right)}{2a\left(x'^2_i - x'^2_p\right)\sqrt{x'^2_i - m^2}\sqrt{x'^2_p - m^2}} \tag{14}$$

for a TE mode coupling to a TE mode,

$$H_{ip} = \frac{\ell_o m k_B \omega}{2ac\sqrt{k_i}\sqrt{k_p}\sqrt{x'^2_p - m^2}} \tag{15a}$$

for a TE mode coupling to a TM mode, and

$$H_{i\varphi}^{-} = \frac{k_B \ell_o \left(k_i x_p^{\,2} - k_p x_i^{\,2}\right)}{2a\sqrt{k_i k_p}\left(x_p^{\,2} - x_i^{\,2}\right)} \tag{15b}$$

for a TM mode coupiing to a TM mode.

Since equations 10 form a first order system of linear ordinary differential equations, the solution to equations 10 can be determined by assuming a solution of the form[5]

$$f_i(z) = \sum_{i=1}^{n} c_i \xi_i e^{\gamma_i z} \tag{16}$$

where n is twice the number of modes, γ is an eigenvalue of the linear system, ξ is the eigenvector corresponding to γ, and c is a complex number needed to match the boundary conditions.

In most cases, only two modes need to be considered: the mode of interest and the next nearest mode with the same azimuthal mode number. In the two mode case, the solution of the differential equations reduces to finding the eigenvalues and eigenvectors of the corresponding matrix.

$$\begin{bmatrix} -i\Delta_1 & -iG_1 & 0 & iH_{12} \\ iG_1 & i\Delta_1 & -iH_{12} & 0 \\ 0 & iH_{12} & -i\Delta_2 & -iG_2 \\ -iH_{12} & 0 & iG_2 & i\Delta_2 \end{bmatrix} \begin{pmatrix} a_1^+ \\ a_1^- \\ a_2^+ \\ a_2^- \end{pmatrix} = \gamma \begin{pmatrix} a_1^+ \\ a_1^- \\ a_2^+ \\ a_2^- \end{pmatrix} \tag{17}$$

The four eigenvalues of this system are

$$\gamma_1 = \pm\frac{1}{2}\sqrt{-\Delta_1^2-\Delta_2^2+G_1^2+G_2^2+2H_{12}^2+\sqrt{\left(\Delta_1^2-\Delta_2^2-G_1^2+G_2^2\right)^2+4H_{12}^2\left[(G_1+G_2)^2-(\Delta_1-\Delta_2)^2\right]}}\text{, and}$$

$$\gamma_2 = \pm\frac{1}{2}\sqrt{-\Delta_1^2-\Delta_2^2+G_1^2+G_2^2+2H_{12}^2-\sqrt{\left(\Delta_1^2-\Delta_2^2-G_1^2+G_2^2\right)^2+4H_{12}^2\left[(G_1+G_2)^2-(\Delta_1-\Delta_2)^2\right]}}$$

and the corresponding general solution is

$$\begin{pmatrix} a_1^+(z) \\ a_1^-(z) \\ a_2^+(z) \\ a_2^-(z) \end{pmatrix} = c_1 \begin{pmatrix} \left(\Delta_2^2-G_2^2+\gamma_1^2\right)(\gamma_1-i\Delta_1)+S^2(-\gamma_1+i\Delta_2) \\ \left[G_1\left(\Delta_2^2-G_2^2+\gamma_1^2\right)+G_2S^2\right] \\ S\left[G_2(\gamma_1-i\Delta_1)+G_1(\gamma_1-i\Delta_2)\right] \\ S\left[(i\gamma_1+\Delta_1)(\gamma_1+i\Delta_2)+i\left(G_1G_2-S^2\right)\right] \end{pmatrix} e^{i\gamma_1 z} +$$

$$c_2 \begin{pmatrix} \left(\Delta_2^2-G_2^2+\gamma_1^2\right)(-\gamma_1-i\Delta_1)+S^2(\gamma_1+i\Delta_2) \\ \left[G_1\left(\Delta_2^2-G_2^2+\gamma_1^2\right)+G_2S^2\right] \\ S\left[G_2(-\gamma_1-i\Delta_1)+G_1(-\gamma_1-i\Delta_2)\right] \\ S\left[(-i\gamma_1+\Delta_1)(-\gamma_1+i\Delta_2)+i\left(G_1G_2-S^2\right)\right] \end{pmatrix} e^{-i\gamma_1 z} +$$

$$c_3 \begin{pmatrix} S\left[(i\gamma_2+\Delta_1)(\gamma_2+i\Delta_2)+i\left(G_1G_2-S^2\right)\right] \\ S\left[G_2(-\gamma_2-i\Delta_1)+G_1(-\gamma_2-i\Delta_2)\right] \\ i\left[G_2\left(\Delta_1^2-G_1^2+\gamma_2^2\right)+G_1S^2\right] \\ \left(-\Delta_1^2+G_1^2-\gamma_2^2\right)(\gamma_2+i\Delta_2)+S^2(\gamma_2+i\Delta_1) \end{pmatrix} e^{i\gamma_2 z} +$$

$$c_4 \begin{pmatrix} S\left[(-i\gamma_2+\Delta_1)(-\gamma_2+i\Delta_2)+i\left(G_1G_2-S^2\right)\right] \\ S\left[G_2(+\gamma_2-i\Delta_1)+G_1(+\gamma_2-i\Delta_2)\right] \\ i\left[G_2\left(\Delta_1^2-G_1^2+\gamma_2^2\right)+G_1S^2\right] \\ \left(-\Delta_1^2+G_1^2-\gamma_2^2\right)(-\gamma_2+i\Delta_2)+S^2(-\gamma_2+i\Delta_1) \end{pmatrix} e^{-i\gamma_2 z} \qquad 18$$

The constants c_1 through c_4 are determined by the boundary conditions and are, in general, complex. For the case where mode 1 is incident on the reflector, the constants are determined by the following relation:

$$\begin{pmatrix} a_1^+(0) \\ a_1^-(L) \\ a_2^+(0) \\ a_2^-(L) \end{pmatrix} = \begin{pmatrix} 1 \\ 0 \\ 0 \\ 0 \end{pmatrix}, \tag{19}$$

where L is the length of the rippled section. Due to the complexity of the solution of equation 19, constants c_1 through c_4 are determined numerically. The power reflectivity of the corrugated section in the mode of interest is $\left|\frac{a_1^-(0)}{a_1^+(0)}\right|^2$, and the reflection into the stray mode is $\left|\frac{a_2^-(0)}{a_1^+(0)}\right|^2$.

III. EXAMPLES

As an example of the application of the methods in this paper, we have calculated the reflection and mode conversion for a TF_{11} mode Bragg reflector at 85 GHz and a TE_{61} mode Bragg reflector at 100 GHz. The TE_{11} mode is of interest for applications where the electron beam is centered on the axis of the waveguide, as in some cyclotron auto-resonance masers (CARMs) and free-electron lasers (FELs).

In the TE_{11} mode design, the ripple depth is 0.1 mm. The dominant competing mode in the reflector section is the TM_{11} mode, because it is the mode with the same azimuthal index with the closest cutoff frequency to that of the TE_{11} mode. The corrugated section is 15 cm long in order to achieve 93% reflectivity. Table 1 contains the parameters for the TE_{11} mode reflector. Figure 2 illustrates the spatial dependence of the 85 GHz fields in the reflector. For the TE_{11} and TM_{11} mode both the forward and backward wave powers are shown. Since the mode conversion in this reflector is weak, the TM_{11} mode powers have been multiplied by ten. The TE_{11} mode, for which the Bragg resonance is satisfied, has a wave amplitude that decreases exponentially with distance in the reflector. The spatial dependance of the TM_{11} mode is oscillatory. Figure 3 shows the frequency dependence of the reflection and transmission of the corrugated section. The peak in the TM_{11} reflected power occurs where the Bragg resonance is satisfied for the TE_{11} to TM_{11} reflection. In this design the presence of the TM mode has little effect on the reflection coefficient. Even so, the conversion of TE_{11} to TM_{11} provides a mode-mix of 90% TE mode and 10% TM mode in the transmitted signal.

Reflector design mode	TE_{11}
Upstream reflector length	4 cm
Corrugation period	1.7 mm
Corrugation amplitude	0.1 mm
Center frequency	85 GHz
Power reflectivity	
TE_{61}	93.3%%
TM_{61}	0.5%
Output mode	
TE_{61}	5.6%
TM_{61}	0.6%

Table 1. Design parameters of an 85 GHz TE11 Bragg Reflector

The second example is a TE_{61} mode Bragg reflector for cyclotron autoresonance maser (CARM) applications. Cyclotron masers often use annular electron beams, primarily because annular electron beams can be formed using magnetron-injection guns (MIGs). Consequently, resonators designed for operation in whispering-gallery modes are of interest for CARMs. Table 2 presents the parameters of a TE_{61} mode reflector for a CARM oscillator resonator. Figure 4 shows the frequency dependance of the reflection and mode conversion in the reflector. In order to keep mode conversion to a tolerable level, the amplitude of the corrugations, ℓ_0 was kept to 0.12 mm. Because the coupling in the TE_{61} mode is strong, the reflector is comprised of only 24 periods. Consequently the width of the resonance is wide enough to overlap with the TE_{61} to TM_{61} Bragg resonance. If the mode conversion is ignored when the reflectivity is calculated, the calculated reflectivity is 93%. The resulting mode conversion causes approximately one half of the output power is expected to be in the TM_{61} mode.

Figure 3 displays a Bragg reflector with little mode conversion, while Figure 4 depicts a reflector where the mode conversion is important. Mode conversion is more prevalent in the whispering-gallery case than in the fundamental-mode case for two reasons. First, the coupling coefficients are strongest for the whispering-gallery modes. Second, the frequency separation between the TE-TE Bragg resonance and the nearest TE-TM Bragg resonance is somewhat smaller for higher-order modes. When the resonance regions overlap, as they do in figure 4, mode conversion can be large.

Reflector design mode	TE_{61}
Reflector length	4 cm
Corrugation period	1.7 mm
Corrugation amplitude	0.12 mm
Center frequency	100 GHz
Power reflectivity	
TE_{61}	89.6%
TM_{61}	2.0%
Output mode	
TE_{61}	4.0%
TM_{61}	4.4%

Table 2. Design parameters of a TE_{61} Bragg Reflector

IV. CONCLUSIONS

A set of general equations for the coupled modes of rippled-wall resonators has been derived. These equations, which can be readily solved using matrix-algebra techniques, demonstrate that unless they are designed carefully, Bragg reflectors and resonators can suffer from mode conversion that will reduce the cavity Q-factor for the desired mode, and possibly prevent oscillation in that mode.

V. ACKNOWLEDGEMENT

This work was supported by the U. S. Office of Naval Research.

VI. REFERENCES

[1] V. L. Bratman, G. G. Denisov, N. S. Ginzburg, and M. I. Petelin, "FEL's with Bragg Reflection Resonators: Cyclotron Autoresonance Masers Versus Ubitrons," *IEEE Journal of Quantum Electronics,* Vol. QE-19, no. 3, pp. 282-296, March, 1983.

[2] L. Solymar, "Spurious Mode Generation in Nonuniform Waveguide.," *I.R.E. Trans. Micro. Theory Tech.,* pp. 379, 1959.

[3] R. B. McCowan, A. W. Fliflet, S. H. Gold, V. L. Granatstein, and M. C. Wang, " Design of a waveguide resonator with rippled-wall reflectors for a 100 GHz CARM oscillator experiment.," *International Journal of Electronics,* Vol. 65, no. 3, pp. 463-475, 1988.

[4] A. J. Palmer, "Coupled-Mode Theory of Overmoded Cylindrical Metal Bragg-Reflectors. ," *I.E.E.E. J. Quant. Electron.,* Vol. 23, no. 65, .

[5] W. E. Boyce and R. C. Diprima, *Elementary Differential Equations and Boundary Value Problems,* New York, John Wiley and Sons, pp. 312, 1977.

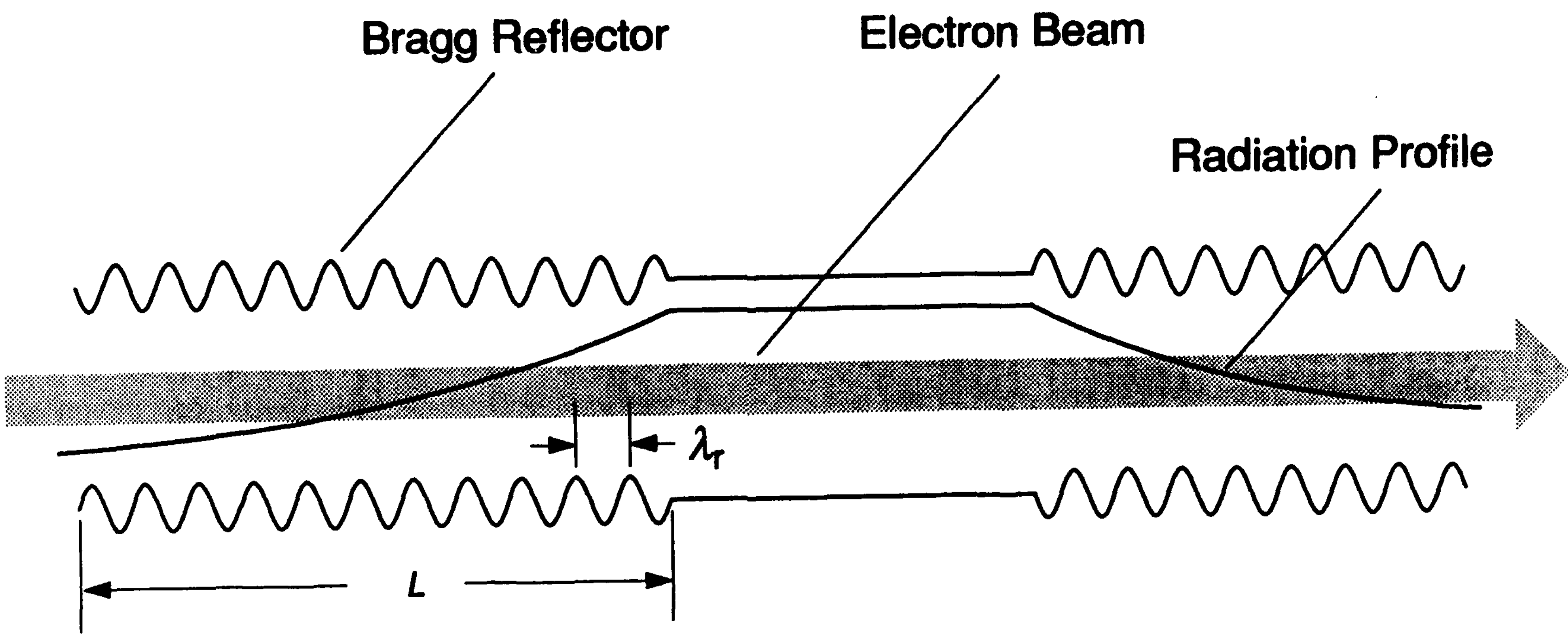

Fig. 1 — A schematic of a CARM oscillator cavity using Bragg reflectors

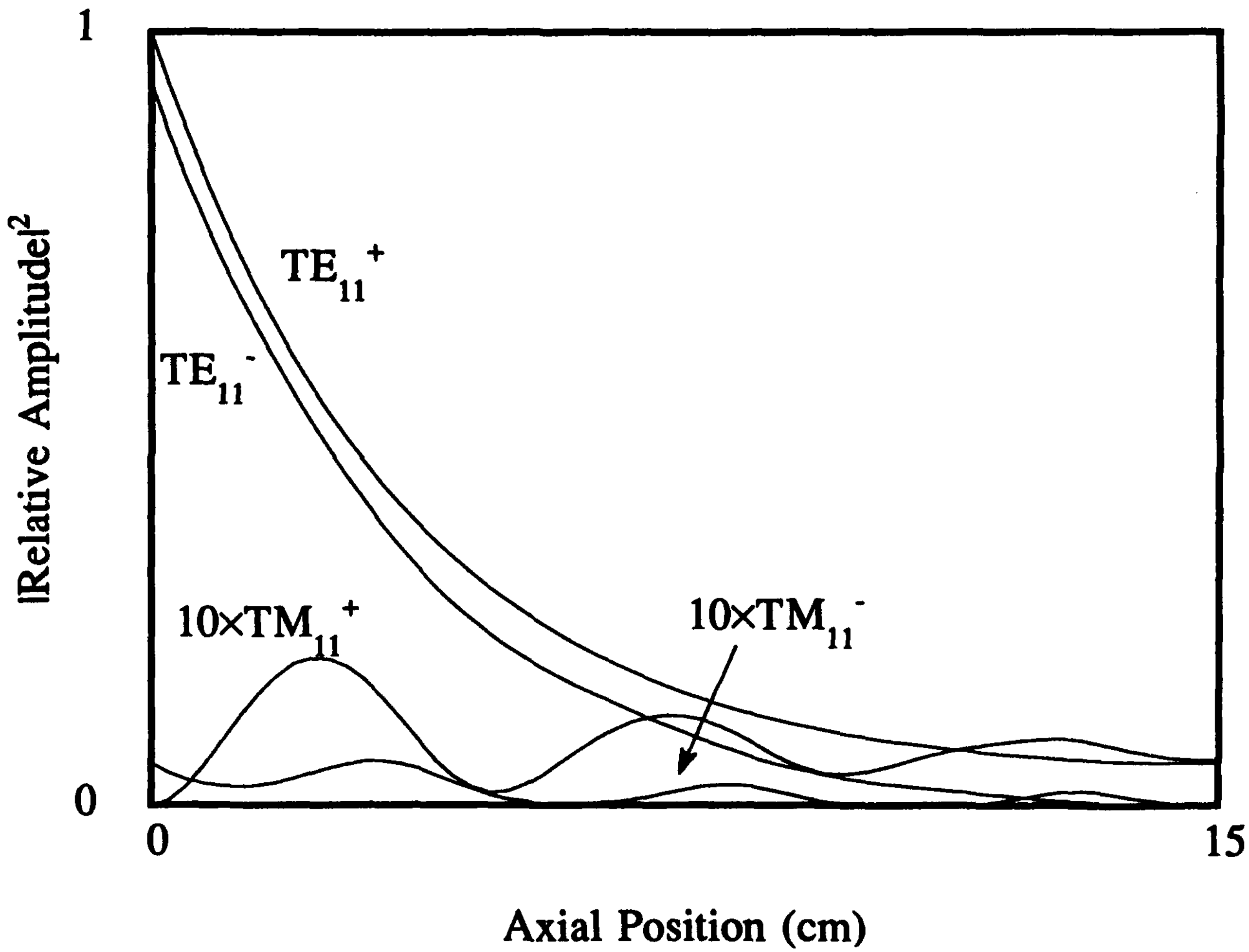

Fig. 2 — The spatial dependence of the TE_{11} and TM_{11} electric fields in an 85 GHz Bragg reflector designed to operate in the TE_{11} mode. The TM_{11} mode amplitudes are multiplied by 10. The dimensions of this reflector are shown in Table 1.

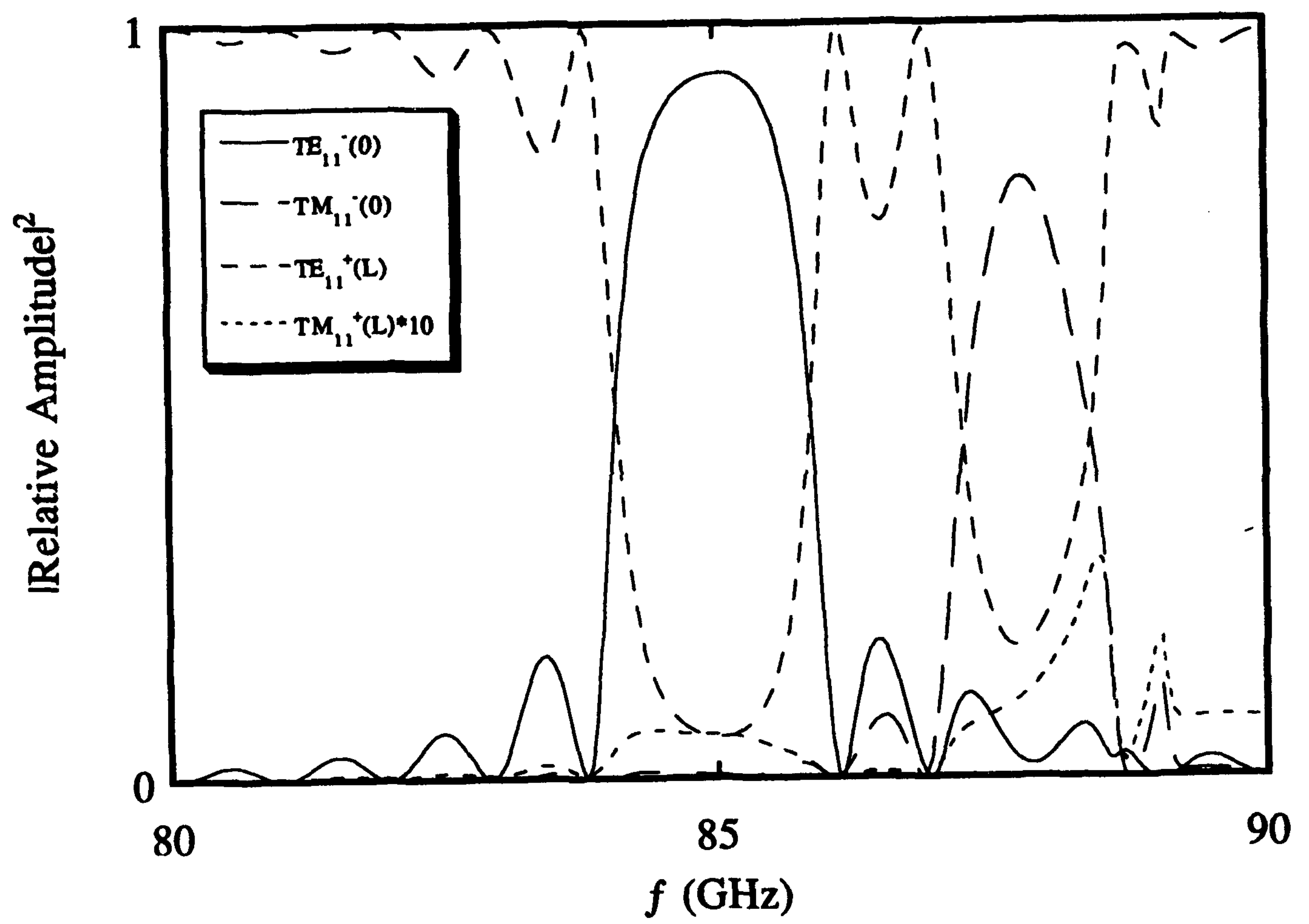

Fig. 3 — The frequency dependence of reflection and transmission in the 85 GHz Bragg reflector

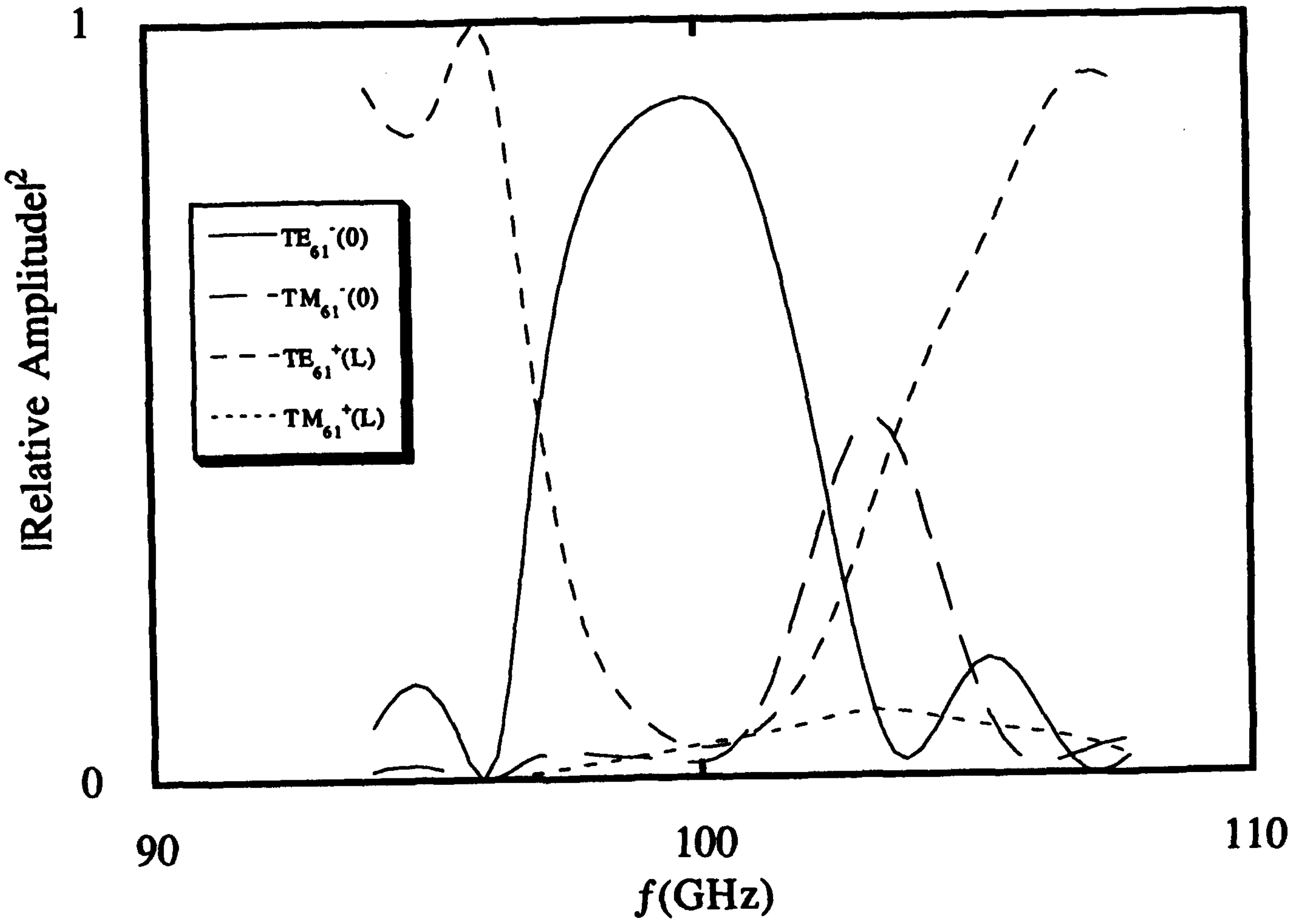

Fig. 4 — The frequency dependence of reflection and transmission in the TE_{61} and TM_{61} modes in a Bragg reflector designed to operate at 100 GHz in the TE_{61} mode. The parameters for this reflector are shown in Table 2.